COVID-19 lockdowns cause global air pollution declines

Zander S. Venter[a,1], Kristin Aunan[b], Sourangsu Chowdhury[c], and Jos Lelieveld[c,d]

[a]Terrestrial Ecology Section, Norwegian Institute for Nature Research, 0349 Oslo, Norway; [b]Center for International Climate Research, 0318 Oslo, Norway; [c]Department of Atmospheric Chemistry, Max Planck Institute for Chemistry, 55128 Mainz, Germany; and [d]Climate and Atmosphere Research Center, The Cyprus Institute, 1645 Nicosia, Cyprus

Edited by Akkihebbal R. Ravishankara, Colorado State University, Fort Collins, CO, and approved July 9, 2020 (received for review April 10, 2020)

The lockdown response to coronavirus disease 2019 (COVID-19) has caused an unprecedented reduction in global economic and transport activity. We test the hypothesis that this has reduced tropospheric and ground-level air pollution concentrations, using satellite data and a network of >10,000 air quality stations. After accounting for the effects of meteorological variability, we find declines in the population-weighted concentration of ground-level nitrogen dioxide (NO_2: 60% with 95% CI 48 to 72%), and fine particulate matter ($PM_{2.5}$: 31%; 95% CI: 17 to 45%), with marginal increases in ozone (O_3: 4%; 95% CI: −2 to 10%) in 34 countries during lockdown dates up until 15 May. Except for ozone, satellite measurements of the troposphere indicate much smaller reductions, highlighting the spatial variability of pollutant anomalies attributable to complex NO_x chemistry and long-distance transport of fine particulate matter with a diameter less than 2.5 μm ($PM_{2.5}$). By leveraging Google and Apple mobility data, we find empirical evidence for a link between global vehicle transportation declines and the reduction of ambient NO_2 exposure. While the state of global lockdown is not sustainable, these findings allude to the potential for mitigating public health risk by reducing "business as usual" air pollutant emissions from economic activities. Explore trends here: https://nina.earthengine.app/view/lockdown-pollution.

air quality | COVID-19 confinement | emissions | nitrogen dioxide | particulate matter

In many developing nations, economic growth has exacerbated air pollutant emissions, with severe consequences for the environment and human health. Long-term exposure to air pollution including fine particulate matter with a diameter less than 2.5 μm ($PM_{2.5}$) and ozone (O_3) is estimated to cause ∼8.8 million excess deaths annually (1, 2), while nitrogen dioxide (NO_2) results in 4 million new pediatric asthma cases annually (3). Despite the apparent global air pollution "pandemic," anthropogenic emissions continue to increase in most developing and some developed nations (4–6).

The major ambient (outdoor) air pollution sources include power generation, industry, traffic, and residential energy use (4, 7). With the rapid emergence of the novel coronavirus disease 2019 (COVID-19), and, in particular, the government-enforced lockdown measures aimed at containment, economic activity associated with transport and mobility has come to a near-complete standstill in many countries (8). Lockdown measures have included partial or complete closure of international borders, schools, and nonessential businesses and, in some cases, restricted citizen mobility (*SI Appendix*, Fig. S1) (9). The associated reduction in traffic and industry has both socioeconomic and environmental impacts which are yet to be quantified. In parallel to the societal consequences of the global response to COVID-19, there is an unprecedented opportunity to estimate the short-term effects of economic activity counterfactual to "business as usual" on global air pollution and its relation to human health.

Here we test the hypothesis that COVID-19 lockdown events between January and the middle of May 2020 were associated with declines in ambient NO_2, O_3, and $PM_{2.5}$ air pollutant concentrations. Country-specific lockdowns are defined by the average date of policy restrictions on mobility, workplace closure, and stay-at-home advisories (10). We use satellite data to provide a global perspective on atmospheric pollutant dynamics, but, to quantify air pollution anomalies relevant to public health, we utilize ground-level measurements from >10,000 air quality stations in 34 countries, after accounting for meteorological variations.

Results and Discussion

General Air Pollution Changes. Before accounting for meteorological variability, we observed declines in ground-level NO_2 (36% population-weighted mean with interquartile range [IQR] of 26%) and $PM_{2.5}$ (31%; IQR: 50%) concentrations recorded by air quality stations across 34 countries during 2020 (1 January to 15 May) relative to a 3-y average for the same dates (Fig. 1). In contrast, O_3 increased by 105% (77% IQR). Satellite measurements of tropospheric pollutant concentrations over the inhabited areas also reveal declines in NO_2 (15%; IQR: 27%) and increases in O_3 (4%; IQR: 6%; *SI Appendix*, Figs. S3 and S4) relative to 2019 averages. Measures of aerosol optical depth (AOD, a proxy for $PM_{2.5}$) declined by 4.7% (35% IQR). Therefore, ground-level and total column tropospheric trends in pollutants show a correspondence in the direction of change but not necessarily the magnitude of change. This is likely because tropospheric pollutant concentrations may be significantly diluted relative to ground-level concentrations, due to mixing and transport in mesoscale weather systems. This is particularly likely because the satellite data have not been adjusted for confounding meteorological effects. For instance, elevated AOD may be a product of long-distance aerosol transport and not ground-level sources of $PM_{2.5}$ (11). The same is true for satellite-measured O_3, which is strongly influenced by its generally increasing abundance above the boundary layer, especially during winter.

Significance

The global response to the COVID-19 pandemic has resulted in unprecedented reductions in economic activity. We find that, after accounting for meteorological variations, lockdown events have reduced the population-weighted concentration of nitrogen dioxide and particulate matter levels by about 60% and 31% in 34 countries, with mixed effects on ozone. Reductions in transportation sector emissions are largely responsible for the NO_2 anomalies.

Author contributions: Z.S.V., K.A., S.C., and J.L. designed research; Z.S.V. performed research; Z.S.V. analyzed data; and Z.S.V., K.A., S.C., and J.L. wrote the paper.

The authors declare no competing interest.

This article is a PNAS Direct Submission.

[1]To whom correspondence may be addressed. Email: zander.venter@nina.no.

This article contains supporting information online at https://www.pnas.org/lookup/suppl/doi:10.1073/pnas.2006853117/-/DCSupplemental.

First published July 28, 2020.

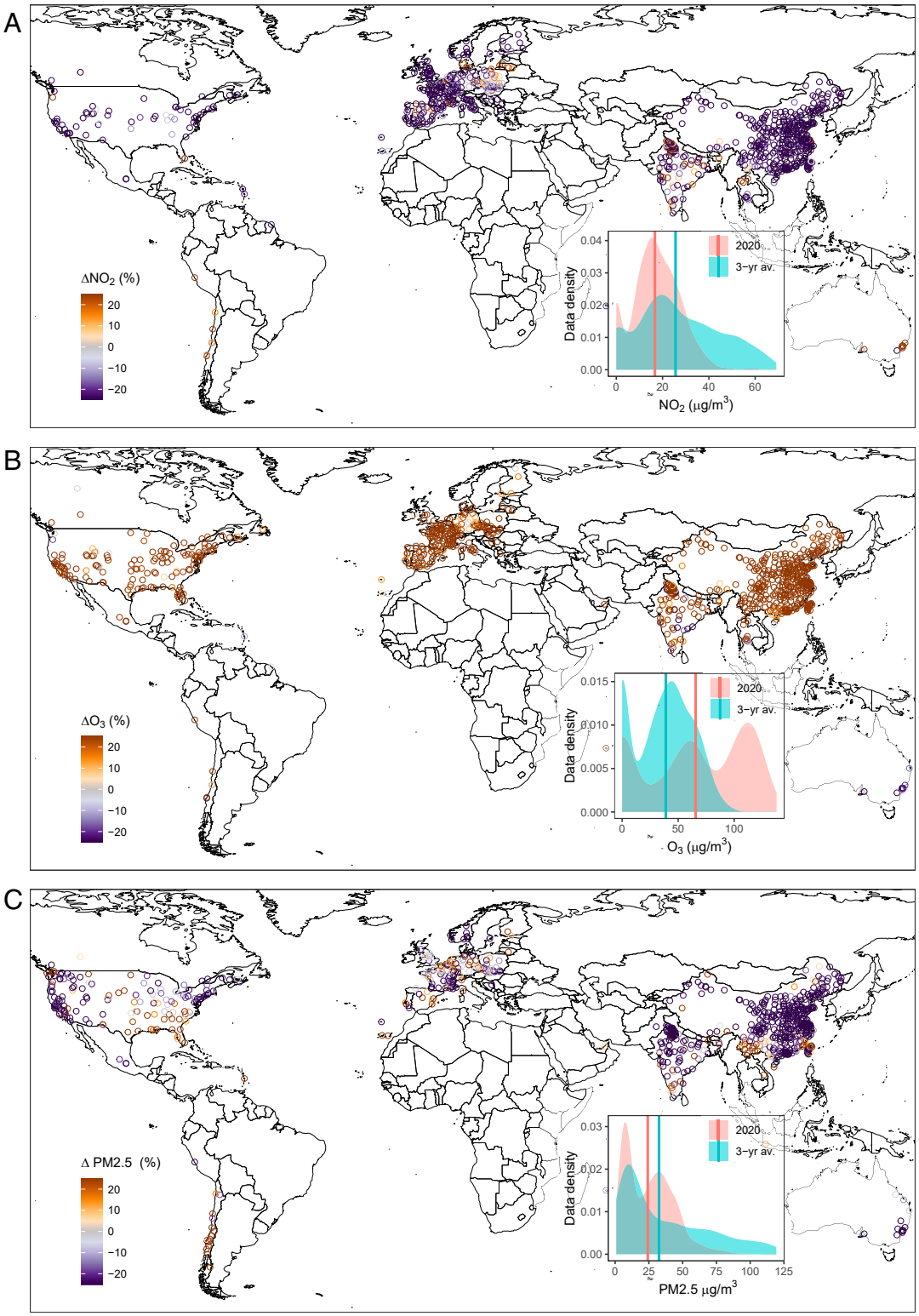

Fig. 1. Global distribution of 2020 ground-level air pollution anomalies. Ground station measures of NO_2 (*A*), O_3 (*B*), and $PM_{2.5}$ (*C*) anomalies are mapped. Anomalies are defined as deviations in 2020 January–May averages from 3-y baseline levels for the same dates and are not corrected for weather variability. *Insets* show data density distributions for baseline and 2020 periods with median values as vertical lines.

The simple comparison of 2020 January–May averages to 3- or 1-y baseline values (Fig. 1 and *SI Appendix*, Figs. S3 and S4) does not isolate the COVID-19 lockdown effect for two reasons. Firstly, lockdowns were implemented over different dates across the globe, and, therefore, averaging over January–May smooths over the country-specific lockdown effects. Secondly, local up to synoptic-scale weather patterns (temperature, humidity, precipitation, vertical mixing, and advection) can significantly affect

ground-level pollutant concentrations (12, 13). Although measuring 2020 changes relative to previous years partially controls for this, it does not fully account for anomalous weather during 2020 that may have confounded any observable effect of COVID-19 lockdowns. Therefore, we used historical relationships between weather and daily pollutant time series in a regression model to estimate what the pollutant levels would have been during lockdown dates. The COVID-19 lockdown effect was then defined as the difference between observed and weather benchmark pollutant levels (*SI Appendix*, Fig. S2). We used ground-level measurements because they are more sensitive to emission source changes and are more relevant to human exposure and health risk.

Weather-Corrected Air Pollution Changes during Lockdown. As of 15 May 2020, the 34 countries considered had been in lockdown for an average of 62 d, with China (113 d) and Italy (84 d) undergoing the longest lockdowns and Mexico undergoing the shortest (50 d; *SI Appendix*, Fig. S1). During lockdown dates, ground-level NO_2 concentrations were, on average, 60% (population-weighted mean with 95% CI: 48 to 72%) lower than those we would have expected given the prevailing weather and time of year (weather-corrected benchmark; Figs. 2*A* and 3*A*). Similarly, $PM_{2.5}$ declined by 31% (17 to 45%), whereas O_3 increased by 4% (−2 to 10%; Figs. 2 and 3). In absolute terms (Fig. 3*A*), this equates to an 11 $\mu g{\cdot}m^{-3}$ (9 $\mu g{\cdot}m^{-3}$ to 14 $\mu g\ m^{-3}$) decline in NO_2 and a 12 $\mu g{\cdot}m^{-3}$ (7 $\mu g{\cdot}m^{-3}$ to 18 $\mu g{\cdot}m^{-3}$) decline in $PM_{2.5}$. The 4 $\mu g{\cdot}m^{-3}$ increase in O_3 (1 $\mu g{\cdot}m^{-3}$ to 8 $\mu g{\cdot}m^{-3}$) was lower in magnitude and less significant. These results mirror the direction of change found in the general trends for uncorrected ground-level (Fig. 1) and satellite-derived pollutant dynamics (*SI Appendix*, Figs. S3 and S4). They also corroborate preliminary (not peer-reviewed) findings from studies in China (14), Spain (15), and the United States (16) which have documented local declines in pollutant concentrations during lockdown.

Globally, the timing of the deviation from benchmark levels for NO_2 was remarkably coincident with the start of lockdown (Fig. 2 and *SI Appendix*, Fig. S5). This timing was strongly evident for $PM_{2.5}$ in China (decline of 16 $\mu g{\cdot}m^{-3}$) and India (decline of 15 $\mu g{\cdot}m^{-3}$), but less so for $PM_{2.5}$ over European countries. This may be because $PM_{2.5}$ is significantly influenced by long-distance atmospheric transport, and, therefore, the local effects of economic activity over Europe may have been diluted or even counteracted (17). As an example, in March, easterly winds carried desert dust across Europe from west Asia, which resulted in a temporal increase of AOD (18). Moreover, some $PM_{2.5}$ sources, including agriculture and energy production, were not disrupted by lockdown policy restrictions. This is also evidenced in the two notable outlier countries exhibiting increases in $PM_{2.5}$, namely, Thailand and Australia (Fig. 3). There, the increases are largely attributable to the recent wildfires and associated smoke aerosol levels that have overwhelmed the effect of reduced economic and transport activity (19, 20).

We find that the global NO_2 and $PM_{2.5}$ anomalies associated with lockdowns normalized after about 2 mo (Fig. 2). This normalization occurred in early April over China (*SI Appendix*, Fig. S5), which is consistent with the release of lockdown on 8 April over Wuhan province, the epicenter of the COVID-19 pandemic. NO_2 concentrations normalize during late April and early May over European countries, including Italy, Spain, and the United Kingdom (*SI Appendix*, Fig. S5). This is likely a signal of increasing economic activity coincident with the gradual easing of lockdown restrictions around the world after countries have successfully "flattened the curve" of COVID-19 infections (21).

Explaining the Spatial Variation in Change. Despite the overall average decline in air pollution during lockdown, there was substantial variation between countries, in terms of both the direction and magnitude of change (Fig. 3). The declines in NO_2 were relatively ubiquitous over space (28 out of 34 countries; Fig. 3); however, O_3 and $PM_{2.5}$ anomalies were more variable. We posit that this spatial variation is likely due to a combination of 1) unaccounted for meteorological and environmental factors that affect ambient air pollution chemistry or 2) country-specific differences in the way lockdown regulations influenced pollution emission sources across economic sectors.

Our weather benchmark models were not able to explain all of the temporal variance in NO_2 ($R^2 = 0.52$), O_3 ($R^2 = 0.59$), and $PM_{2.5}$ ($R^2 = 0.34$) (*SI Appendix*, Table S1). This is not surprising, given that pollutants like O_3 are affected by nonlinear chemical interactions with volatile organic compounds (VOCs) and NO_x, mediated by mesoscale and urban canopy circulation patterns (22). For instance, the emission decline of NO_x (= NO + NO_2), mostly as NO, could lead to reduced local titration of O_3 (reaction of NO with O_3). The O_3 titration effect is relevant locally and within the planetary boundary layer, whereas, farther downwind, photochemical O_3 formation, with a catalytic role of NO_x, is a more important factor. For example, in China, the population-weighted O_3 is found to increase with decreasing NO_2 across the lockdown; this indicates predominance of a VOC-limited regime in China, whereas reduction in population-weighted O_3 with decrease in NO_2 in India suggests a NO_x-limited regime prevailing there (*SI Appendix*, Fig. S5).

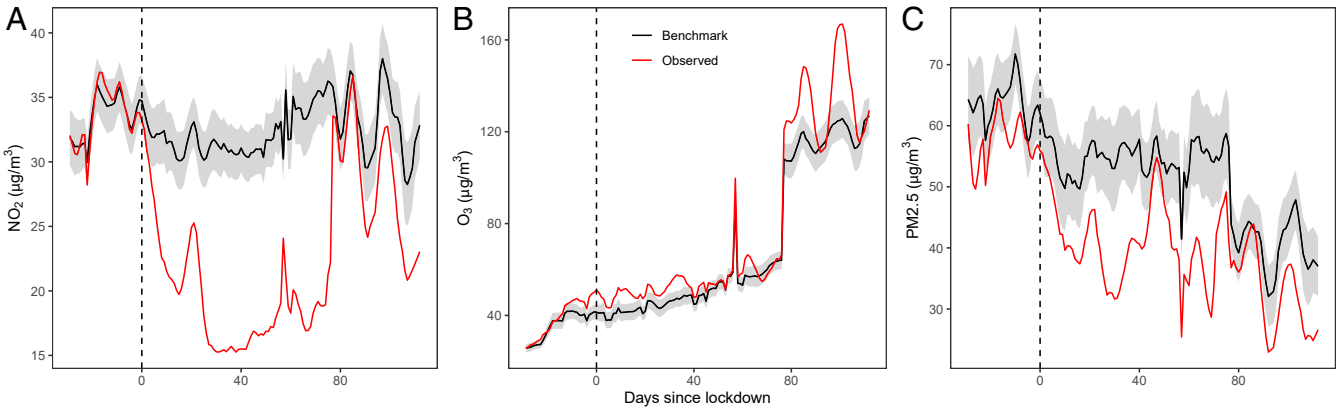

Fig. 2. Lockdown ground-level air pollution anomalies relative to weather benchmarks for NO_2 (*A*), O_3 (*B*), and $PM_{2.5}$ (*C*). The daily population-weighted average ($n = 34$ countries) ambient pollutant concentrations observed 1 mo before and up to 15 May after lockdowns are plotted in red. Benchmark levels which represent expected concentrations considering time of year and prevailing weather are plotted in black with 95% CIs.

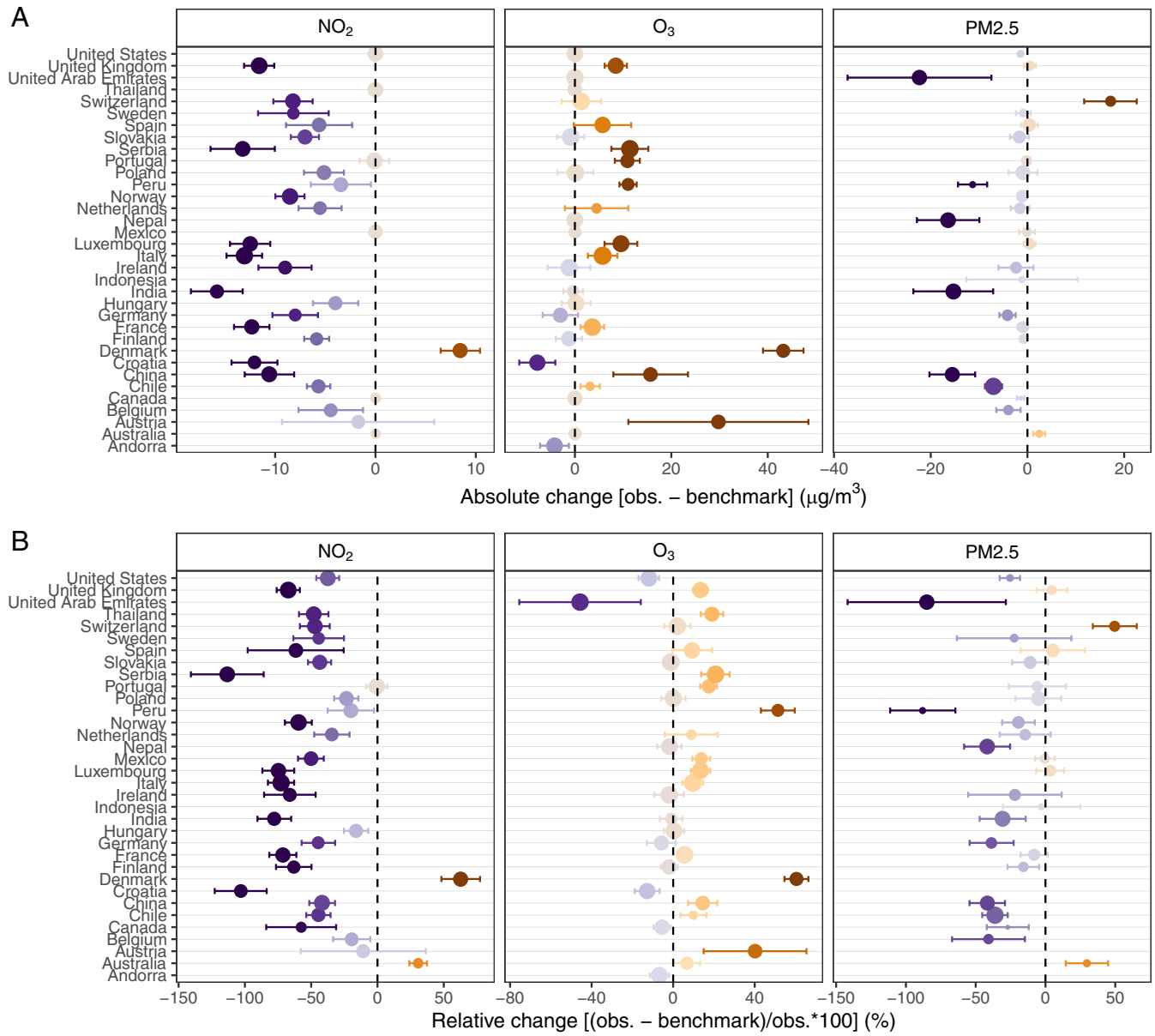

Fig. 3. Country-specific ground-level lockdown air pollution anomalies. The difference between observed (obs.) lockdown ambient pollutant concentrations and those predicted by the weather benchmark model (trained on 2017–2019 data) are plotted for 34 countries (points) with 95% CIs (error bars). Larger points represent regression models with greater R^2 values. Both absolute (*A*) and relative (*B*) changes are presented.

Note that lockdown impacts on NO_2, which has an atmospheric lifetime of about a day, are clearly discernible locally, whereas those on O_3 with a lifetime of several weeks are affected by long-distance transport associated with specific weather patterns. Further, O_3 photochemistry in temperate latitudes during the February/March period is still slow due to low solar irradiation, whereas, at lower latitudes, pollutant O_3 buildup can be significant.

The alternative explanation for the spatial variability in pollutant changes during lockdown is that confinement regulations had varying effects on emission sources between countries. Recent analyses of the 17% decline in CO_2 emissions during lockdowns have indicated substantial variability between economic sectors (23), with the largest declines taking place in the surface transport sector. Sector allocations of CO_2 emissions vary between countries. For example, the transport sector contributes 8% toward CO_2 emissions in China, whereas, in the United Kingdom, allocation is 4 times higher (23). Therefore, one might expect large variations in emission declines (particularly for NO_2) between countries, given that the lockdowns brought about the greatest change in the transportation sector.

We explored nationally aggregated citizen mobility datasets published by Google (https://www.google.com/covid19/mobility/) and Apple (https://www.apple.com/covid19/mobility/) and found a significant association between country-specific NO_2 declines and reductions in work commutes ($P < 0.05$; Fig. 4*A*) and vehicle driving activity ($P < 0.05$; Fig. 4*B*). There were no significant relationships for O_3 and $PM_{2.5}$ anomalies. This suggests NO_2 has a stronger coupling to land transportation and small-business activity declines during lockdown compared to O_3 and $PM_{2.5}$. In many countries, $PM_{2.5}$ is more strongly linked to residential energy use, power generation, and agriculture (7). Given that walking and cycling are attributes of social distancing measures

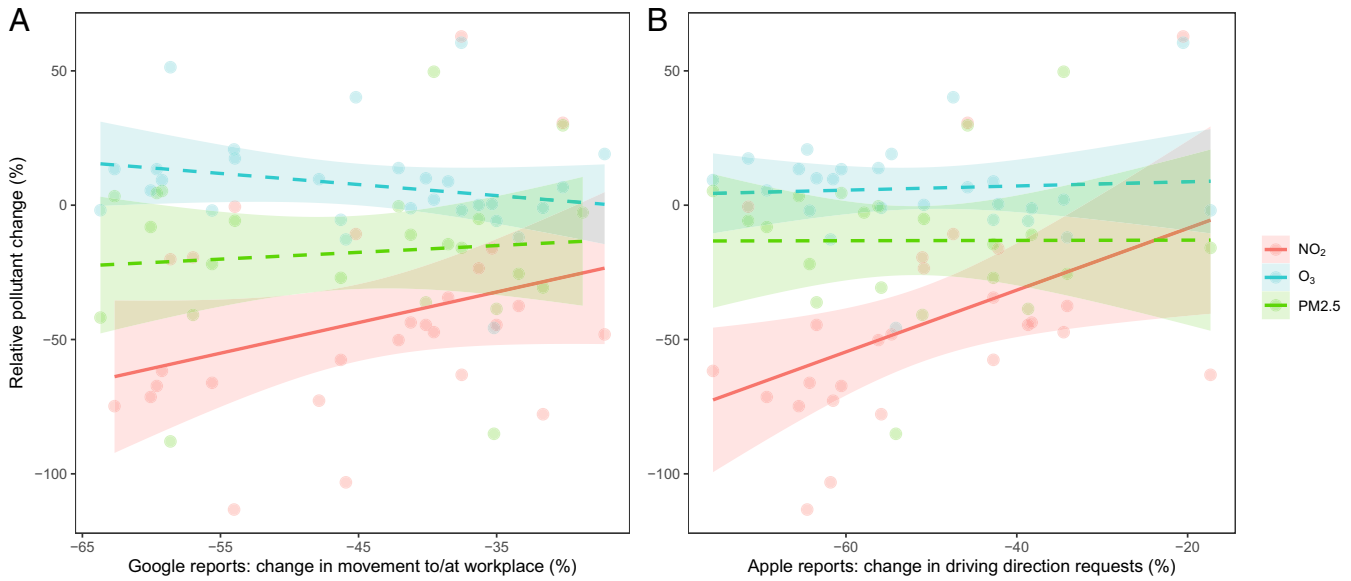

Fig. 4. Lockdown mobility changes relative to ground-level air pollution anomalies. Country-specific ambient air pollution anomalies (observed relative to weather benchmark levels) are regressed on two measures of lockdown-induced citizen mobility declines derived from Google (*A*) and Apple (*B*). Significant (solid) and nonsignificant (dashed) linear regression lines are plotted for each pollutant. Each point represents a country's aggregated value (n = 34).

(24) that are expected to continue for some time (25), reduced NO_2 emissions and therefore exposure levels may be sustained over the near future.

Implications

Reducing economic activity to levels equivalent to a lockdown state may be impractical, yet maintaining "business as usual" clearly exacerbates global pollutant emissions and ambient exposure levels. Our study documents the dramatic short-term effect of global reductions in transport and economic activity on reducing ground-level NO_2 and $PM_{2.5}$, with mixed effects on O_3 concentrations. Short-term epidemiological analyses suggest that pollutant reductions may have offset COVID-19 deaths (14, 26, 27); however, the full extent to which this is true remains to be seen. In some settings where household (indoor) air pollution from solid fuel use is widespread, overall exposure may have increased as a result of lockdown policies (28). As the pandemic plays out, empirical data will emerge to fill in the knowledge gaps and uncertainties associated with the air pollution health burden attribution. Nevertheless, finding means to curb air pollutant emissions remains important, and here we provide empirical evidence at a global scale for a coupling between vehicle transport reduction and declining ambient NO_2 concentrations. This provides justification for city-level initiatives to promote public transport systems as well as pedestrian and cycling activity. Finding economically and socially sustainable alternatives to fossil fuel use in industries, transportation, and power plants, and cleaner fuels for use in households, are additional means of reaching the pollutant declines we have observed during the global response to COVID-19 (29, 30).

Materials and Methods

In brief, the methodological workflow (*SI Appendix*, Fig. S2) described below involves collecting satellite and ground station air pollution time series data to estimate anomalies during the 2020 COVD-19 period relative to different baseline levels. We collected satellite data to provide a global perspective of pollutant trends over regions where there is a scarcity of ground air quality stations. However, we focus on weather-corrected ground station data because ambient pollutant concentrations are more relevant to public health than satellite-derived tropospheric column concentrations. Regression models are used to correct for the potential effects of weather-related variations on ground-level pollutant levels during lockdown. The sample of countries used in each step varies dependent on the data availability. Results for ground station data cover 34 countries, while satellite data cover 48 countries.

Satellite Data. All remote sensing data analyses were conducted in the Google Earth Engine platform for geospatial analysis and cloud computing (31). All data were extracted at a global scale and aggregated to the population-weighted mean for each country. Population data were obtained for 2020 from the Gridded Population of the World v4 dataset (32). Data outside of inhabited areas (ocean, freshwater, desert, etc.) were excluded from the analysis using the Global Human Settlement Layer produced by the European Joint Research Centre which defines inhabited rural and urban terrestrial areas (33). We did this because our main hypothesis was linked to human exposure, and, therefore, we aimed at pollution measures that were relevant to inhabited land surfaces.

We collected nitrogen dioxide (NO_2) and ozone (O_3) data from the Tropospheric Monitoring Instrument (TROPOMI), onboard the Sentinel-5 Precursor satellite (34). TROPOMI has delivered calibrated data since July 2018 from its nadir-viewing spectrometer measuring reflected sunlight in the visible, near-infrared, ultraviolet, and shortwave infrared. Recent work has shown that TROPOMI measurements are well correlated to ground measures of NO_2 (35, 36). We filtered out pixels that are fully or partially covered by clouds, using 0.3 as a cutoff for the radiative cloud fraction. As a proxy for atmospheric $PM_{2.5}$, we collected AOD data from the cloud-masked MCD19A2.006 Terra and Aqua Multi-angle implementation of Atmospheric Correction collection (37) derived from the Moderate Resolution Imaging Spectroradiometer (MODIS). This dataset has been successfully used to map ground-level $PM_{2.5}$ concentrations (38, 39). Global median composite images for NO_2, O_3, and AOD were then calculated for the months of January to May in 2019 and 2020.

Ground Station Data. Although satellite data have the advantage of wall-to-wall global coverage, there are some drawbacks: 1) TROPOMI does not extend back far enough to obtain an adequate baseline measure with which to compare 2020 concentrations; 2) MODIS and TROPOMI collect information within either the total (O_3 and AOD) or tropospheric (NO_2) column which does not necessarily reflect pollutant levels experienced on the ground. Therefore, we also collected NO_2, O_3, and $PM_{2.5}$ data from >10,000 in situ air quality monitoring stations to supplement the satellite data. These data were accessed from the OpenAQ Platform and originate from government- and research-grade sources. See https://openaq.org/#/?_k=d8f1zb for a list of sources. Despite the reliability of the sources, we inspected

pollutant time series for each country and removed spurious outliers in the data with z scores (40) exceeding an absolute value of 3 (within 3 SDs from the mean). Following quality control, we were left with data representing 34 countries. When aggregating data to country level, we used population-weighted means based on the population density within 10 km of each ground station.

Quantifying Air Pollution Anomalies. We used two approaches to quantify air pollution anomalies coincident with COVID-19 during January to May 15, 2020. We refer to these as 1) the Jan-May differential and 2) the lockdown differential (*SI Appendix*, Fig. S2). For the Jan-May differential, we calculated average pollutant levels for January–May each year between 2017 and 2020. The differential was defined as the difference between 2020 values and the average of those for a 3-y baseline (2017–2019). For satellite data, the baseline was the 2019 January–May average due to limited temporal extent of TROPOMI data; however, for ground stations, we considered a 3-y (2017–2019) average for the January–May period.

Air pollution anomalies measured with the Jan-May differential approach may smooth over the effect of COVID-19 given that country-specific lockdowns or mitigation actions occurred at different times. For instance, China went into lockdown in January, whereas the majority of lockdowns in other countries occurred in March (*SI Appendix*, Fig. S1). Therefore, we attempted to isolate the effect of COVID-19 mitigation measures by calculating lockdown pollutant levels for each country separately. We utilized a dataset that consolidates national policy regulations relating to COVID-19 confinement measures (10). The start of lockdown was calculated separately for each country as the average date on which policies for stay-at-home restrictions, mobility restrictions, and workplace closures were announced (*SI Appendix*, Fig. S1).

Air pollution anomalies measured during lockdowns are not necessarily attributable to reduced economic activity, but may be an artifact of meteorological variability coincident with the onset of COVID-19. Therefore, we adopted a weather benchmark modeling approach to predict what the expected air pollution levels for 2020 lockdown dates should have been given the prevailing weather conditions and time of year. We used multiple linear regression as a modeling framework after testing both Random Forest and generalized linear models which had lower predictive accuracy based on assessing model performance by predicting against a withheld validation dataset. We built separate linear regression models for each country and pollutant type, where daily pollutant concentrations were regressed on a number of explanatory variables including temperature, humidity, precipitation, wind speed, day of year, day of week, week of year, and month of year. Weather data were downloaded from the Global Forecast System of the National Centers for Environmental Prediction between January 2017 and 15 May 2020. We calculated the *sin* and *cos* component of the day, week, and month variables to account for their cyclical nature. Using models trained on historical data (before 1 January 2020), we predicted the expected pollutant levels for lockdown dates. The modeled differential is then the difference between this predicted benchmark value and the observed pollutant concentrations during lockdown (*SI Appendix*, Fig. S2). This differential can be attributed to COVID-19 mitigation measures with greater confidence than simple comparisons with 3-y baseline values.

Data Availability. Data and scripts used to produce this analysis are available at this GitHub repository: https://github.com/NINAnor/covid19-air-pollution. Explore data from the present manuscript interactively here: https://nina.earthengine.app/view/lockdown-pollution.

ACKNOWLEDGMENTS. Thanks go to Samantha Scott Venter for assistance with collection of country-specific lockdown data. Thanks go to the OpenAQ community for making air quality data open access. K.A. was supported by funding from the European Union's Horizon 2020 research and innovation program under Grant Agreement 820655 (EXHAUSTION). We are grateful for the effort contributed by the reviewers toward improving the manuscript.

1. R. Burnett *et al*., Global estimates of mortality associated with long-term exposure to outdoor fine particulate matter. *Proc. Natl. Acad. Sci. U.S.A.* **115**, 9592–9597 (2018).
2. J. Lelieveld *et al*., Loss of life expectancy from air pollution compared to other risk factors: A worldwide perspective. *Cardiovasc. Res.*, 10.1093/cvr/cvaa025 (2020). Correction in: *Cardiovasc. Res.* **116**, 1334 (2020).
3. P. Achakulwisut, M. Brauer, P. Hystad, S. C. Anenberg, Global, national, and urban burdens of paediatric asthma incidence attributable to ambient NO_2 pollution: Estimates from global datasets. *Lancet Planet. Health* **3**, e166–e178 (2019).
4. M. Crippa *et al*., Gridded emissions of air pollutants for the period 1970–2012 within EDGAR v4.3.2. *Earth Syst. Sci. Data* **10**, 1987–2013 (2018).
5. R. M. Hoesly *et al*., Historical (1750–2014) anthropogenic emissions of reactive gases and aerosols from the Community Emissions Data System (CEDS). *Geosci. Model Dev.* **11**, 369–408 (2018).
6. C. Li *et al*., India is overtaking China as the world's largest emitter of anthropogenic sulfur dioxide. *Sci. Rep.* **7**, 14304 (2017).
7. J. Lelieveld, J. S. Evans, M. Fnais, D. Giannadaki, A. Pozzer, The contribution of outdoor air pollution sources to premature mortality on a global scale. *Nature* **525**, 367–371 (2015).
8. J. Cohen, K. Kupferschmidt, Strategies shift as coronavirus pandemic looms. *Science* **367**, 962–963 (2020).
9. E. Pepe *et al*., COVID-19 outbreak response: A first assessment of mobility changes in Italy following national lockdown. medRxiv:2020.03.22.20039933 (7 April 2020).
10. T. Hale, S. Webster, A. Petherick, T. Phillips, B. Kira, Oxford COVID-19 Government Response Tracker. https://www.bsg.ox.ac.uk/research/research-projects/coronavirus-government-response-tracker#data. Accessed 15 July 2020.
11. F. Dentener, T. Keating, H. Akimoto, Convention on Long-range Transboundary Air Pollution, "Hemispheric transport of air pollution 2010: Part A-ozone and particulate matter" (United Nations, 2010).
12. J. Dawson, Quiet weather, polluted air. *Nat. Clim. Chang.* **4**, 664–665 (2014).
13. D. J. Jacob, D. A. Winner, Effect of climate change on air quality. *Atmos. Environ.* **43**, 51–63 (2009).
14. K. Chen, M. Wang, C. Huang, P. L. Kinney, P. T. Anastas, Air pollution reduction and mortality benefit during the COVID-19 outbreak in China. *Lancet Planet. Health* **4**, e210–e212 (2020).
15. A. Tobías *et al*., Changes in air quality during the lockdown in Barcelona (Spain) one month into the SARS-CoV-2 epidemic. *Sci. Total Environ.* **726**, 138540 (2020).
16. B. Bekbulat *et al*., PM2.5 and ozone air pollution levels have not dropped consistently across the US following societal covid response. ChemRxiv:12275603.v2 (17 May 2020).
17. R. B. Khuzestani *et al*., Quantification of the sources of long-range transport of $PM_{2.5}$ pollution in the Ordos region, Inner Mongolia, China. *Environ. Pollut.* **229**, 1019–1031 (2017).
18. X. Querol *et al*., Monitoring the impact of desert dust outbreaks for air quality for health studies. *Environ. Int.* **130**, 104867 (2019).
19. C. E. Reid *et al*., Associations between respiratory health and ozone and fine particulate matter during a wildfire event. *Environ. Int.* **129**, 291–298 (2019).
20. S. Sambhi, Forest fires rage in northern Thailand. *Eco-Business*, 16 April 2020. https://www.eco-business.com/news/forest-fires-rage-in-northern-thailand/. Accessed 24 May 2020.
21. A. P. Balasa, COVID–19 on lockdown, social distancing and flattening the curve–A review. *Eur. J. Bus. Manag. Res.* **5** (2020).
22. M. E. Marlier, A. S. Jina, P. L. Kinney, R. S. DeFries, Extreme air pollution in global megacities. *Curr. Clim. Change Rep.* **2**, 15–27 (2016).
23. C. Le Quéré *et al*., Temporary reduction in daily global CO_2 emissions during the COVID-19 forced confinement. *Nat. Clim. Change* **10**, 647–653 (2020).
24. Z. Venter, D. Barton, V. Gundersen, H. Figari, M. Nowell, Urban nature in a time of crisis: Recreational use of green space increases during the COVID-19 outbreak in Oslo, Norway. SocArXiv:10.31235/osf.io/kbdum (9 May 2020).
25. S. M. Kissler, C. Tedijanto, E. Goldstein, Y. H. Grad, M. Lipsitch, Projecting the transmission dynamics of SARS-CoV-2 through the postpandemic period. *Science* **368**, 860–868 (2020).
26. E. Conticini, B. Frediani, D. Caro, Can atmospheric pollution be considered a co-factor in extremely high level of SARS-CoV-2 lethality in Northern Italy? *Environ. Pollut.* **261**, 114465 (2020).
27. X. Wu, R. C. Nethery, B. M. Sabath, D. Braun, F. Dominici, Exposure to air pollution and COVID-19 mortality in the United States. medRxiv:2020.04.05.20054502 (27 April 2020).
28. H. Shen *et al*., Increased air pollution exposure among the Chinese population during the national quarantine in 2020. EarthArXiv:10.31223/osf.io/6d9rn (15 June 2020).
29. J. Lelieveld *et al*., Effects of fossil fuel and total anthropogenic emission removal on public health and climate. *Proc. Natl. Acad. Sci. U.S.A.* **116**, 7192–7197 (2019).
30. S. Chowdhury *et al*., Indian annual ambient air quality standard is achievable by completely mitigating emissions from household sources. *Proc. Natl. Acad. Sci. U.S.A.* **116**, 10711–10716 (2019).
31. N. Gorelick *et al*., Google Earth engine: Planetary-scale geospatial analysis for everyone. *Remote Sens. Environ.* **202**, 18–27 (2017).
32. Center for International Earth Science Information Network–CIESIN–Columbia University, Gridded Population of the World, Version 4 (GPWv4): Population Density, Revision 11. https://doi.org/10.7927/H49C6VHW. Accessed 15 July 2020.

33. M. Pesaresi, S. Freire, Data from "GHS Settlement grid following the REGIO model 2014 in application to GHSL Landsat and CIESIN GPW v4-multitemporal (1975-1990-2000-2015)." Joint Research Centre Data Catalogue. http://data.europa.eu/89h/jrc-ghsl-ghs_smod_pop_globe_r2016a. Accessed 15 July 2020.
34. J. P. Veefkind *et al*., TROPOMI on the ESA sentinel-5 precursor: A GMES mission for global observations of the atmospheric composition for climate, air quality and ozone layer applications. *Remote Sens. Environ.* **120**, 70–83 (2012).
35. D. Griffin *et al*., High-Resolution mapping of nitrogen dioxide with TROPOMI: First results and validation over the Canadian oil sands. *Geophys. Res. Lett.* **46**, 1049–1060 (2019).
36. A. Lorente *et al*., Quantification of nitrogen oxides emissions from build-up of pollution over Paris with TROPOMI. *Sci. Rep.* **9**, 20033 (2019).
37. A. Lyapustin, Y. Wang, S. Korkin, D. Huang, MODIS Collection 6 MAIAC algorithm. *Atmos. Meas. Tech.* **11**, 5741–5765 (2018).
38. Y. Zheng, Q. Zhang, Y. Liu, G. Geng, K. He, Estimating ground-level PM2.5 concentrations over three megalopolises in China using satellite-derived aerosol optical depth measurements. *Atmos. Environ.* **124**, 232–242 (2016).
39. S. Chowdhury *et al*., Tracking ambient PM2.5 build-up in Delhi national capital region during the dry season over 15 years using a high-resolution (1 km) satellite aerosol dataset. *Atmos. Environ.* **204**, 142–150 (2019).
40. D. Cousineau, S. Chartier, Outliers detection and treatment: A review. *Int. J. Psychol. Res. (Medellin)* **3**, 58–67 (2010).